Pulsed Laser-Induced Photochemical Decomposition of GaAs(110) Studied with Time-Resolved Photoelectron Spectroscopy Using Synchrotron Radiation

J. P. Long, S. S. Goldenberg,[a] and M. N. Kabler
Naval Research Laboratory, Washington, D.C. 20375
(Received 26 August 1991)

Cleaved GaAs surfaces decompose under weak pulsed-laser irradiation, leading to the formation of metallic Ga islands. The reduction of band-bending nonuniformities in photoemission spectra acquired during the laser pulses, in concert with new core-level fitting techniques which treat broadened spectra, permits a detailed analysis. A decomposition rate consistent with a two-step photochemical excitation process is measured. The surface remains largely intact on an atomic scale, but is increasingly unable to support excited surface states as decomposition proceeds.

PACS numbers: 79.60.−i, 73.20.−r, 82.50.−m

The surfaces of III-V semiconductors can be decomposed by heat at temperatures well below the melting point. For GaAs, for example, temperatures of 800–900 K are required [1]. In this Letter we show that decomposition of clean GaAs(110) surfaces and the consequent formation of metallic Ga islands can occur near room temperature through a photon-activated process. Using repeated laser pulses we have produced Ga islands with fluences as low as 1 mJ/cm^2, which cause a peak temperature rise during the pulse of no more than 13 K. This decomposition is thus predominantly photochemical and not thermal. Although we have so far investigated only cleaved GaAs and GaP, with positive results, it is likely the basic process is related to a variety of optical effects observed in the processing and degradation of compound semiconductors.

Primary evidence for the decomposition is the appearance of ~100-Å-diam metallic Ga islands dispersed over the surface after it has been irradiated with 5-ns copper vapor laser pulses (510-nm wavelength). The relative coverage of Ga islands is measured *in situ* with photoelectron spectroscopy through a distinct metallic component in the Ga 3*d* core level and through a corresponding metallic Fermi edge in valence-band spectra. The islands are also observed directly in a scanning electron microscope (SEM).

We have developed new experimental and analysis techniques which have proved crucial for characterizing certain aspects of the decomposition process. Photoemission spectra recorded *during* the laser pulses are significantly narrowed because the surface photovoltage (SPV) reduces electrostatic nonuniformities, thus demonstrating that the broadening of core-level spectra from the decomposed surface originates primarily not from chemical disorder, but from nonuniform band bending. These inhomogeneities are accounted for in a heuristic but justifiable fashion in new core-level line fitting routines which yield purely statistical residuals and which permit a more accurate measure of the surface and bulk covalent intensities and extraction of the weak metallic Ga component. The fluence dependence of the fitted metallic component, when calibrated against the volume of metallic Ga in SEM micrographs, reveals dissociation kinetics consistent with a two-step mechanism. Finally, photoemission from laser-excited surface states using synchrotron radiation addresses the nonequilibrium electron dynamics of these surfaces.

The experiments were performed at the National Synchrotron Light Source, Brookhaven National Laboratory, as previously detailed [2,3]. Photoelectron spectra were resolved with a commercial double-pass cylindrical mirror analyzer. A Gaussian system resolution of 0.25 eV FWHM obtains. Laser pulses arriving at a 6-kHz repetition rate were focused to 2 mm FWHM, concentric with the 1-mm synchrotron spot. Time-resolved measurements were made when the storage ring was operating with a single circulating electron bunch, the subnanosecond synchrotron pulse from which was overlapped temporally with the laser pulse. A time-resolved spectrum was built up by gating on this pulse and averaging over many laser pulses.

Both *n*-type (2×10^{16} to 2×10^{18} cm^{-3} Si) and *p*-type (6×10^{17} to 2×10^{19} cm^{-3} Zn) GaAs bars (~5×5-mm^2 cross section) were mounted with indium to a water-cooled block. Mirrorlike surfaces were selected after cleaving at pressures below 2×10^{-10} torr. The sample temperature was obtained by summing the average rise with the calculated [4] peak rise during the pulse and is approximately 13 °C above room temperature per mJ/cm^2 of incident laser fluence. The average rise was determined with thermocouples and corrected [5] for the laser spot's underfilling of the sample cross section.

The evolution of the surface with laser dose is shown in Fig. 1, which compares Ga and As 3*d* core levels recorded before and after a dose of 60 kJ/cm^2 delivered with 3.9-mJ/cm^2 pulses. The weak satellite at a binding energy of 18.5 ± 0.1 eV arises from metallic Ga islands. Its growth with laser dose correlates with the growth of weak metallic emission with a stable cutoff coinciding, within experimental error, with the Fermi edge measured from a gold foil. The least-squares fits, which account for inhomogeneous broadening as described below, separate the

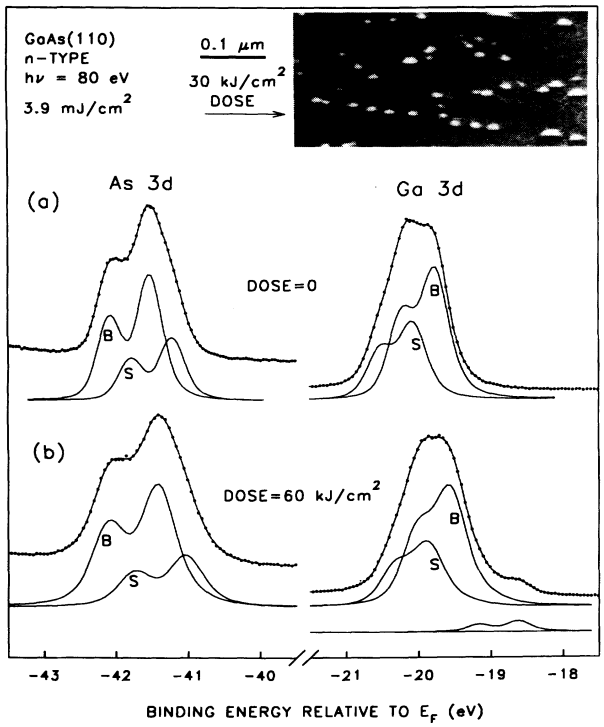

FIG. 1. Data and fits for core-level spectra measured (a) before and (b) after laser-induced decomposition. *B* and *S* label bulk and surface components. The metallic Ga fit is displaced downward. (Polynomial background fits are not shown.) SEM micrograph depicts view from 20° grazing angle.

spectra into the bulk and surface covalent spin-orbit doublets [6]. The fits for the laser doses reported here show that the ratios of surface to bulk intensities for both species decrease by only (10–15)% after dosing, even when the Ga equivalent of several (110) layers resides in islands. Thus the local atomic structure associated with the (110) surface relaxation seems to be retained over most of the surface. Surface stoichiometry is unaffected, as reflected in the constant ratio of Ga to As intensities for the GaAs components. These facts, together with the absence of new components in the As spectra, suggest that the As which had been bound to the liberated Ga has desorbed. Desorbed As was measured at larger (15 mJ/cm^2) fluences with a relatively insensitive quadrupole mass analyzer.

Many SEM micrographs were made for a variety of surfaces. The micrograph in Fig. 1 exhibits a surface exposed under conditions identical to Fig. 1(b) but with a dose of 30 kJ/cm^2. The isolated, 150-Å-diam Ga islands were uniformly dispersed over the center of the laser spot but occasionally followed lines evidently associated with unresolved cleavage steps.

Time-resolved photoemission spectra from the band-gap region reveal not only the growth of a metallic Fermi edge associated with the Ga islands but also transient emission from electrons excited by the laser into the surface-state pocket at $\bar{X}$ in the surface Brillouin zone and nearly degenerate with the conduction-band minimum. Photoemission from this state was first investigated by Haight and Silberman [7] using a laser as both pump and probe. Its presence, which gives some indication of the quality of the surface, is consistent with the core spectra which show relatively little disturbance to the surface during island production. The emission from $\bar{X}$ does decrease with laser dose, an effect which can be ascribed to depletion of carriers through increased recombination. A degree of laser-induced disorder on interisland regions is indicated by slight increases in fitted Gaussian widths, both in ordinary core spectra (after accounting for inhomogeneities), and in time-resolved spectra narrowed by the SPV discussed below. The broadening, as well as average band bending which was usually ≤ 0.1 eV just after cleaving, grows with dose, even before the spectral signatures of islands are seen.

The conventional line fitting procedure used initially to extract the weak metallic Ga component from core spectra was hampered by the broadening associated with nonuniform band bending. Figure 2 illustrates this effect by contrasting time-resolved, surface-sensitive, Ga 3*d* core-level spectra recorded *between* laser pulses [Fig. 2(a)] after the SPV had effectively decayed and recorded *during* the laser pulse [Fig. 2(b)] when the SPV had substantially reduced band-bending nonuniformities and produced a strikingly narrowed spectrum. Note that it is not necessary to include inhomogeneous broadening in the fits to the SPV-narrowed spectra. As illustrated by the schematic drawing of band bending in Fig. 2, the substrate and metallic components exhibit different SPV shifts, demonstrating that there is larger band bending beneath the Ga islands than the intervening substrate. These results contrast those obtained on Si, where the 2*p* core level was found to shift rigidly on the scale of these measurements [8]. We modified our fitting scheme to account for inhomogeneous broadening by adding to each singlet, modeled as a Voight function [9], a small, asymmetric singlet. The asymmetry was introduced by allowing different widths above and below the singlet's center energy. This approach was tested on theoretical spectra and resulted in fits with residuals as good as the Voight function approximation we employ [9]. The theoretical spectra were broadened using the band-bending distribution obtained from the Poisson solver PISCES [10]. Our results are similar to those of Miyano *et al.* [11] who examined circular islands; for charged cleavage steps or chains of islands (modeled as stripes in PISCES), we find that inhomogeneities can be considerably more pronounced.

Figure 3 summarizes the metallic fraction f_m in the core spectra as a function of laser dose D administered at various fluences using both core and calibrated Fermi-edge data. That the growth curves follow roughly the $D^{2/3}$ dependence illustrated by the dashed line can be understood if most of the metallic Ga resides in thick is-

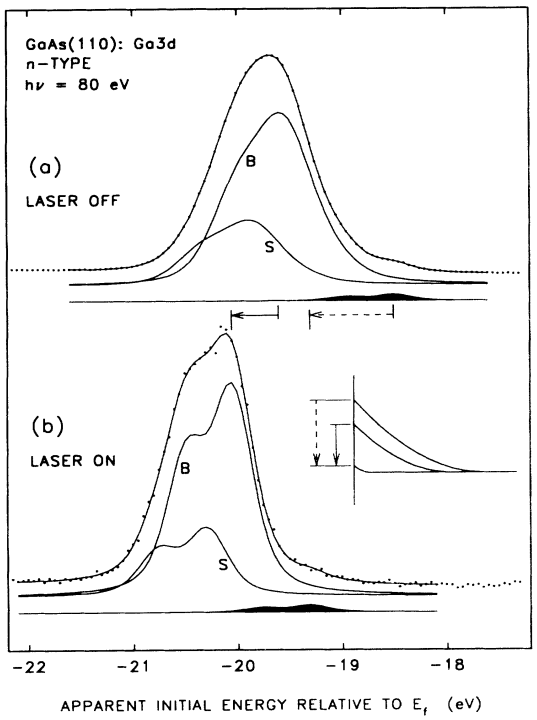

FIG. 2. Ga $3d$ spectra recorded (a) between and (b) during laser pulses of 3.9 mJ/cm^2. Fits to metallic components are shaded and displaced. Arrows superposed on spectra and the schematic of band bending show SPV shift beneath metal (dashed) and intervening substrate (solid).

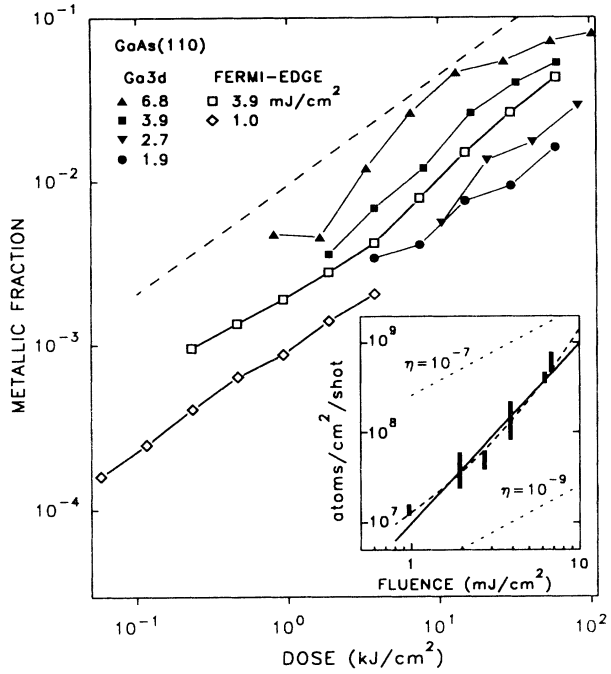

FIG. 3. Laser dose dependence of metallic fraction of the Ga $3d$ core from fits of core spectra and deduced from emission near the Fermi edge. Dashed line is dose $D^{2/3}$. Inset: Fluence dependence of the rate of metal creation. η is the efficiency of metal Ga production in units of Ga atoms per incident photon. Dashed- and solid-line fits support the two-step models discussed in text.

lands. Indeed, the constancy of the metallic Ga $3d$ component with photon energy (photoelectron escape depth) as well as the SEM micrographs show that the islands are thick and that f_m measures the areal coverage of the islands rather than the volume. Therefore, if the volume of metallic Ga produced is proportional to D, at a given fluence, and if the number density of islands is reasonably constant during the dose, then $f_m \propto D^{2/3}$ for three-dimensional island growth. The volume of metallic Ga per unit area of surface is thus taken to be $\propto f_m^{3/2}$, from which a rate of production, Γ, can be determined by calibrating against $f_m^{3/2}$ per shot versus Γ measured directly in a limited number of SEM micrographs. This procedure automatically accounts for the rate dependence [12] of the island size distribution. The inset of Fig. 3 shows Γ (Ga atoms/cm^{2}shot) plotted versus fluence. The absolute values of Γ are accurate within a factor of 3. Also displayed are dotted lines of constant efficiency η, defined as the number of Ga atoms in islands per laser photon incident.

Before considering the kinetics suggested by the superlinear dependence of Γ seen in the inset, we note that once an island forms it concentrates laser intensity within a diameter or so of its periphery in the direction of the optical electric field [13]. This can cause superlinearities in dose and fluence dependences. However, our estimates indicate that these effects are unimportant at the small f_m applicable to this work.

We now consider what atomic processes might be consistent with these data. The most likely sites of the photodecomposition are cleavage steps on the surface, since Ga and As atoms at kinks on the steps are more loosely bound than terrace atoms. The frequent presence of steps and kinks on mirrorlike cleaves has recently been established [14]. The island growth rate might be expected to vary with step density, which may be the source of the variability with cleave which contributes to the two largest error bars in the inset of Fig. 3. Decomposition at steps can be viewed as the inverse of layer-by-layer crystal growth, with the photons providing the dissociation energy.

The dependence of the growth rate Γ on fluence suggests strongly that the rate-limiting process is more complex than the simple release of a single kink atom by one photon. The data can, in fact, be accounted for by a two-step process involving a lifetime-limited intermediate state. If the probability of each step is proportional to fluence F, then the bulk island growth can be linear in dose and $\Gamma \propto F^2$, as shown by the solid line in the inset of Fig. 3. This model is consistent with the data, but the na-

ture of the intermediate state is left uncertain. One possibility is a limited atomic movement or bond rearrangement at a kink site which, if not excited a second time, relaxes back to the original configuration. The dissociation rate might be determined primarily by the motion of either the Ga, the As, or both.

Since to free a Ga or As atom on the surface requires the breaking of at least one bond, it is probable that to provide sufficient energy at least one of the two steps involves direct photon absorption at the site. However, the other step could be initiated by either nonradiative electron-hole recombination, electron or hole trapping, or even the small temperature rise caused by the laser pulse. In the latter case, if the second step is thermally activated, then $\Gamma \propto Fe^{-E/kT}$. Using $T=296+13F$ (F in mJ/cm^2) as previously discussed, we obtain the dashed curve in the Fig. 3 inset, with $E=0.23$ eV. Although the fit appears slightly better than F^2, the difference is not enough to favor the photon-pulse-thermal mechanism. We have compared these simple kinetic models quantitatively with the measured decomposition rate Γ. Relevant parameters such as cross sections σ, intermediate lifetimes τ, and active-site densities N_0 can only be estimated, and a detailed description is unwarranted. Nevertheless, it is important to note that the two-step processes which include one or two direct photon excitations can reproduce the observed Γ with reasonable ranges of parameters. As an illustration, consider the case where both steps rely on direct photon absorption and $\tau < \tau_L$, the laser pulse length. Then the kinetic model gives $\Gamma/F^2 = N_0\sigma_1\sigma_2\tau/\tau_L$, which is measured to be 2×10^{-24} cm^2. If $\sigma_i = 3\times10^{-18}$ cm^{-2}, a typical optical cross section, and $\tau = 10^{-9}$ s, then $N_0 \approx 10^{12}$ cm^{-2}, a density consistent with those measured directly on similarly cleaved samples [14].

Finally, it is interesting to compare these results with the work of Itoh and co-workers, who studied laser-induced surface reconstructions and photodesorption of Ga on GaP [15]. These measurements did not reveal Ga islands. The dependence on laser wavelength, along with small temperature rises, suggested a nonthermal process. Although there are substantial differences between the experiments and interpretations of Itoh and co-workers and ours, it appears that the basic photochemical processes may be similar.

We are grateful to J. Meyer for performing the calculations of instantaneous temperature. This research was carried out in part at the National Synchrotron Light Source, which is sponsored by the U.S. Department of Energy under Contract No. DE-AC02-76CH00016.

---

[a]NRC-NRL Postdoctoral Research Associate. Now with SFA, Inc., Landover, MD 20785.

[1] F. Proix, A. Akremi, and Z. T. Zhong, J. Phys. C **16**, 5449 (1983).

[2] J. P. Long, Nucl. Instrum. Methods Phys. Res., Sect. A **266**, 673 (1988).

[3] S. S. Goldenberg, J. P. Long, and M. N. Kabler, Mater. Res. Soc. Symp. Proc. **201**, 519 (1991).

[4] J. R. Meyer, M. R. Kruer, and F. J. Bartoli, J. Appl. Phys. **51**, 5513 (1980).

[5] H. S. Carslaw and J. C. Jaeger, *Conduction of Heat in Solids* (Oxford Univ. Press, Oxford, 1986), 2nd ed.

[6] T. Miller and T.-C. Chiang, Phys. Rev. B **29**, 7034 (1984).

[7] R. Haight and J. A. Silberman, Phys. Rev. Lett. **62**, 815 (1989).

[8] J. P. Long, H. R. Sadeghi, J. C. Rife, and M. N. Kabler, Phys. Rev. Lett. **64**, 1158 (1990).

[9] Julio Puerta and Pablo Martin, Appl. Opt. **20**, 3923 (1981); errata, Appl. Opt. **22**, 19 (1983).

[10] PISCES-IIB, Stanford University Software Distribution Center, Stanford, CA.

[11] K. E. Miyano, David M. King, C. J. Spindt, T. Kendelewicz, R. Cao, Zhiping Yu, I. Landau, and W. E. Spicer, Phys. Rev. B **43**, 11806 (1991).

[12] J. B. Adams, W. N. G. Hitchon, and L. M. Holzmann, J. Vac. Sci. Technol. A **6**, 2029 (1988).

[13] L. D. Landau and E. M. Lifshitz, *Electrodynamics of Continuous Media* (Addison-Wesley, Reading, 1960).

[14] Y.-N. Yang, B. M. Trafas, R. L. Siefert, and J. H. Weaver, Phys. Rev. B **44**, 3218 (1991).

[15] Y. Nakai, K. Hattori, and N. Itoh, Appl. Phys. Lett. **56**, 1980 (1990); Y. Kumazaki, Y. Nakai, and N. Itoh, Phys. Rev. Lett. **59**, 2883 (1987).

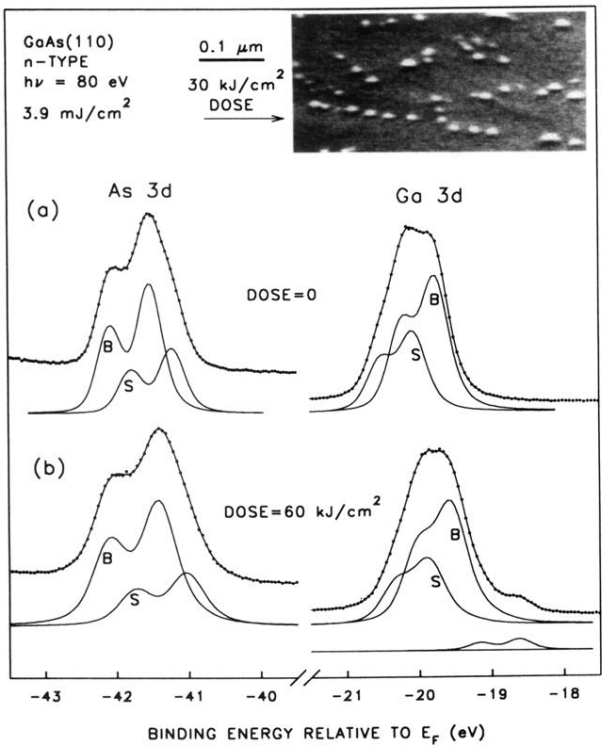

FIG. 1. Data and fits for core-level spectra measured (a) before and (b) after laser-induced decomposition. *B* and *S* label bulk and surface components. The metallic Ga fit is displaced downward. (Polynomial background fits are not shown.) SEM micrograph depicts view from 20° grazing angle.